Technobius Physics, 2024, 2(2), 0014, https://doi.org/10.54355/tbusphys/2.2.2024.0014

Technobius Physics

https://technobiusphysics.kz/

e-ISSN 3007-0147

Article

Cooling and heating innovations: exploring the diverse applications of heat pumps

Aliya Nurbayeva, Karina Mussabekova*

Faculty of Mechanical Engineering, Energy and Information Technologies, Akhmet Baitursynuly Kostanay Regional University, 47 Baytursynov st., Kostanay, Kazakhstan
*Correspondence: karina.mussabekova@mail.ru

Abstract. Heat pumps are versatile and energy-efficient devices that play a crucial role in modern heating, cooling, and refrigeration applications. This abstract provides a concise overview of the diverse applications and benefits of heat pumps across residential, commercial, industrial, and transportation sectors. The abstract discusses the principles of heat pump operation, emphasizing their capability to transfer heat from one location to another using thermodynamic processes. The abstract highlights key applications such as residential heating, ventilation, and air conditioning systems, commercial refrigeration, hot water heating, process cooling, and renewable energy integration. The energy efficiency and environmental benefits of heat pumps are also emphasized, showcasing their potential to reduce carbon emissions and contribute to sustainable energy practices. By understanding the broad scope of heat pump applications outlined in this abstract, researchers, engineers, policymakers, and industry stakeholders can gain insights into the significance of heat pump technology in advancing energy efficiency and addressing climate change challenges.
Keywords: heating, ventilation, air conditioning, temperature control, humidity regulation, energy efficiency.

1. Introduction

Heat pumps have emerged as essential and versatile technologies in modern heating, cooling, and refrigeration applications across residential, commercial, industrial, and transportation sectors [1]. These devices utilize thermodynamic principles to transfer heat from one location to another, providing efficient and environmentally friendly solutions for space conditioning and temperature control [2].

In recent years, the adoption of heat pumps has increased significantly due to their energy efficiency, reduced environmental impact, and versatility in diverse applications [3–6]. This article explores the wide-ranging applications of heat pumps, highlighting their role in residential heating and cooling, commercial HVAC systems, refrigeration, hot water heating, process cooling, and renewable energy integration.

The Peltier effect is based on the principles of thermoelectricity, which involves the conversion of temperature differences into electric voltage (Seebeck effect) and vice versa (Peltier effect) [7–9]. This effect has practical applications in thermoelectric cooling devices, such as portable refrigerators, where it is used for efficient heat pumping without the need for moving parts like compressors, making it a key technology in various industries ranging from consumer electronics to scientific instrumentation (Figure 1).

This effect describes the heating or cooling of a junction of two dissimilar conductors or semiconductors when an electric current is passed through them. When current flows through the junction, heat is either absorbed or released, depending on the direction of the current:

$$\frac{Q}{t} = P_P = \pi * I = \alpha * T * I \quad (1)$$

Where π is the Peltier coefficient, the α is the Seebeck coefficient [10] and T is the absolute temperature. Heat will either be absorbed or released in a homogeneous conductor when an electric current T runs in the direction of a temperature gradient $\frac{dT}{dx}$, depending on the material (Thomson effect):

$$P_T = \tau * I * \frac{dT}{dx} \quad (2)$$

Where τ is the Thomson coefficient. Figure 2 demonstrate a Peltier element is typically made from two different types of semiconductor materials, often bismuth telluride Bi_3Te_3 or other similar materials with high thermoelectric efficiency [11-12]. The semiconductor material is doped to create two types of regions: N-type (electron-rich) and P-type (hole-rich). These regions are arranged to create multiple P-N junctions, which are crucial for the Peltier effect.

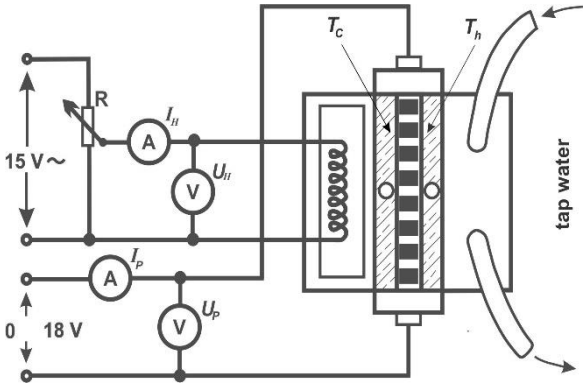

Figure 1 – Configuration to ascertain cooling capability

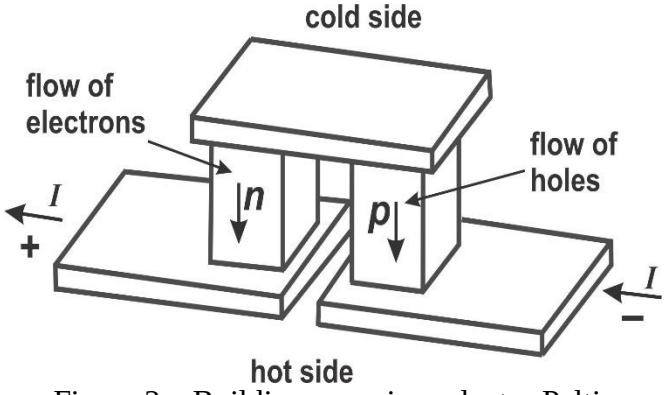

Figure 2 – Building a semi-conductor Peltier element: in actuality, a number of parts are typically connected both thermally and electrically in parallel

Figure 3 is a power balance block diagram for a Peltier component including an illustration of how electrical energy is converted into thermal energy and the cooling effect within the device [13-14].

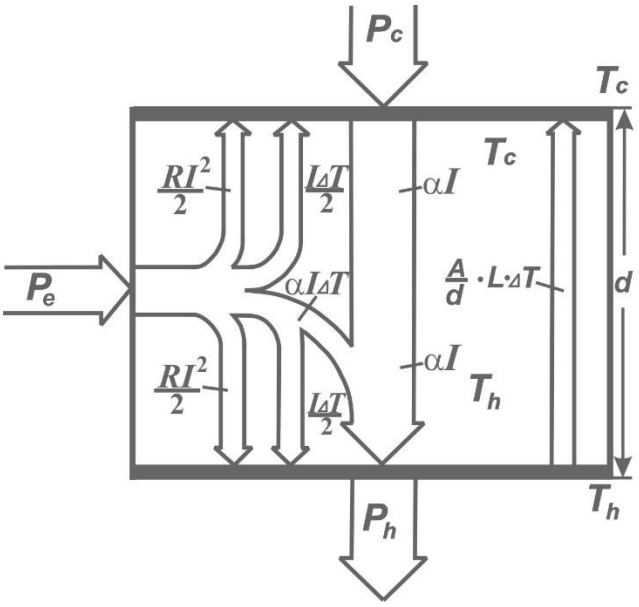

Figure 3 – A Peltier component's power balance flow diagram, that provided relates to the scenario in which $PT > 0$

The Peltier component is powered by an electrical input, typically from a DC power source. The input electrical power is the energy provided to the Peltier device. The Peltier effect occurs at the

junctions of the Peltier device, where heat is either absorbed or released depending on the direction of the electric current. One side of the Peltier device absorbs heat from the surroundings. This side becomes cooler. The other side of the Peltier device rejects heat into the surroundings. This side becomes warmer. The absorbed heat results in cooling of one side of the Peltier device, achieving the desired cooling effect. The rejected heat increases the temperature of the opposite side of the Peltier device. The Peltier device facilitates the transfer of heat from one side to the other, depending on the direction of the electric current. The net effect is the generation of cooling on one side and heating on the other side of the Peltier device, allowing for precise temperature control and thermal management [15-16].

The sign of the Thomson coefficient, the direction of the temperature gradient, and the direction of the current all influence which way heat moves. The Joule effect occurs when an electric current I runs through an isothermal conductor with resistance R:

$$P_J = R * I^2 \tag{3}$$

Heat also transfers from the hot side T_h to the cold side T_C due to heat conduction:

$$P_L = L\frac{A}{d}(T_h - T_C) \tag{4}$$

Where A is the cross-sectional area, d is the thickness of the Peltier component, and L is the conductivity.

By $\Delta T = T_h - T_C$, it can be derived the following for the pump's cold-side heat capacity (also known as its cooling capacity):

$$-P_C = \alpha T_C I \pm \frac{\tau I \Delta T}{2d} - \frac{1}{2} I^2 R - \frac{LA\Delta T}{d} \tag{5}$$

Additionally, regarding the hot side pump's heat capacity:

$$+P_h = \alpha T_h I \pm \frac{\tau I \Delta T}{2d} - \frac{1}{2} I^2 R - \frac{LA\Delta T}{d} \tag{6}$$

The electricity that is provided is:

$$+P_{el} = \alpha \Delta T I \pm \frac{\tau I \Delta T}{2d} - I^2 R = U_p * I_P \tag{7}$$

The objective of this experimental investigation is to explore the operational characteristics of a Peltier heat pump. The study aims to accomplish several specific goals: firstly, to ascertain the cooling capacity of the pump as a variable function of applied current; secondly, to compute the efficiency rating of the heat pump under conditions of maximum cooling output. Additionally, the investigation seeks to determine the heating capacity of the pump and its corresponding efficiency rating under conditions of sustained current and a consistent temperature on the cold side.

Moreover, the study endeavors to establish the time-dependent behaviors of temperature across the hot and cold sides of the heat pump, discerning pertinent relationships between these variables. Specifically, the experiment aims to characterize the temporal evolution of temperature on both sides during operational phases.

Furthermore, an examination of the temperature dynamics during cooling operations is intended, particularly focusing on the air-cooled condition of the hot side of the heat pump. This investigation will provide insights into the thermal behaviors and operational constraints of the Peltier heat pump system in the context of cooling applications.

By understanding the varied applications and benefits of heat pumps, stakeholders in the energy and HVAC industries can make informed decisions about deploying these technologies to achieve energy savings, improve thermal comfort, and contribute to sustainable practices. This article aims to provide a comprehensive overview of heat pump applications, emphasizing their importance in advancing energy-efficient solutions and mitigating climate change challenges.

2. Methods

We have assembled an improved experimental setup for accurate thermal experiments and measurements, which includes: thermogenerator with 2 water baths; flow-through heat exchanger,

which allows for controlled heat exchange processes, crucial for studying fluid dynamics and thermodynamics; an apparatus designed to rapidly cool gases or liquids, providing a means to investigate cooling processes and heat dissipation; heating coil with sockets, that utilized for generating and controlling heat through electrical resistance, enabling varied heat settings for experimental setups.

The installation also included distributor, which used to evenly distribute fluids or gases, ensuring uniformity in experimental conditions; a precision variable resistor (33 Ohm, 3.1A) employed for adjusting current flow in electrical circuits, essential for fine-tuning heating elements; capable of delivering both DC (0-18 V, 0-5 A) and AC (2/4/6/8/10/12/15 V, 5 A) currents, facilitating a wide range of electrical experiments; Power supply, universal DC: 0...18 V, 0...5 A / AC: 2/4/6/8/10/12/15 V, 5 A, four high-precision instruments for measuring voltage (up to 600V AC/DC), current (up to 10A AC/DC), resistance (up to 20 MΩ), capacitance (up to 200 μF), frequency (up to 20 kHz), and temperature (from -20°C to 760°C); A multifunctional timer with precision down to 1/100 second, essential for timing experiments accurately; A powerful device (1800 W) capable of generating controlled streams of hot or cold air for thermal studies; several thermometers calibrated for different temperature ranges (-10°C to +110°C and -10°C to +50°C), crucial for monitoring and recording experimental temperatures; with an internal diameter of 6 mm, used for connecting different components in fluid systems.

All equipment was held by essential's powerful apparatus to fix and stabilise the experimental setups like universal clamp, tripod base, support rod, stainless steel, l = 250 mm, d = 10 mm.; a specialized clamp for securely holding equipment at right angles, ensuring stability during experiments. A variety of heavy-duty connection cords (32 A) in different lengths and colours (red and blue), ensured safe and efficient electrical connections. During the experiment, we used heat conductive paste to increase the thermal conductivity between the surfaces, ensuring efficient heat transfer in the units.

On the cold side, a water bath was erected, and on the hot side, a heat exchanger that allows tap water to flow through was installed. An alternating current heating coil with a resistance of roughly 3 Ohm was submerged in a water-filled bath. Using a rheostat R, the heating power $P_H = U_H * I_H$ was adjusted for each value of current I_P to ensure that there was little to no temperature differential between the hot and cold sides. in which instance the power supplied and the cooling power are exactly identical. The temperatures of the hot side T_h and the cold side Tc were recorded, together with the values of the heater current I_h, voltage U_h, operational current I_P, and voltage U_P.

Then, the heating coil was removed. Now that the operational current was flowing in the opposite direction, the bath water was heated. At constant current I_P, the values of the water's temperature rise (T_W) were noted. Additionally, the temperature rise T_C was measured. Determine the heat capacities of the brass bath C_{BR}, the water C_W, and the copper block C_{CU} using their respective weights or dimensions.

Subsequently, water baths were erected on either side of the heat pump and loaded with uniformly heated water. At a constant current \I_P\, the temperature variations of the two water baths were recorded:

$$T_h = f(t), T_C = f(t), I_p, U_p \quad (8)$$

The air cooler is on the hot side and the water bath is on the cold side in the fourth experiment. In two different regimes—when the cooler is in static atmospheric air and when it is forcefully cooled by a blower—the temperature of the cold side was measured as a function of time.

3. Results and Discussion

By determining the cooling capacity P_C of the pump as a function of the current, it can be assessed how effectively η_C the pump transfers heat from the system it is cooling. The cooling capacity (in watts) provides a quantitative measure of the pump's ability to remove heat, which is

crucial for applications where temperature control is essential (e.g., in HVAC systems, refrigeration, or thermal management of electronic devices).

In the experimental investigation, the cooling capacity P_C of the pump was determined to be 49 W under the condition where the pump current I_P was set at 5 A and the input power P_h equaled the cooling power P_C. This finding represents a quantitative measure of the pump's ability to remove heat from the system at the specified operating parameters. This dependence is presented visually in Figure 4.

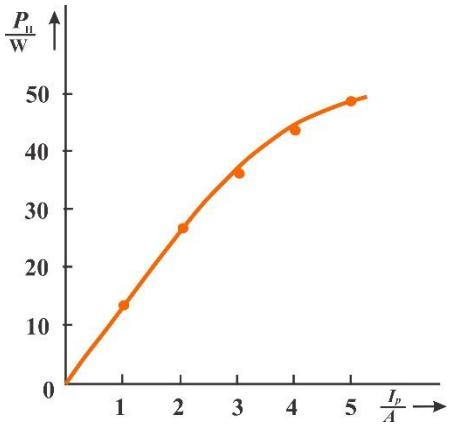

Figure 4 – The relationship between the operating current and pump cooling capacity

Calculated efficiency factor supplied by formula:

$$\eta_C = \frac{P_C}{P_{el}} \tag{9}$$

Using the measured values I_P = 5 A, U_P = 14.2 V and η_C = 0.69 (with $\upsilon_h = \upsilon_C = 20$°C).

Understanding the heating capacity helps evaluate how much heat the pump can generate under specific operating conditions. This information is crucial for assessing the pump's performance in heating applications, such as in thermal management systems or heating devices. A plot of the hot side temperature versus time is shown in Figure 5.

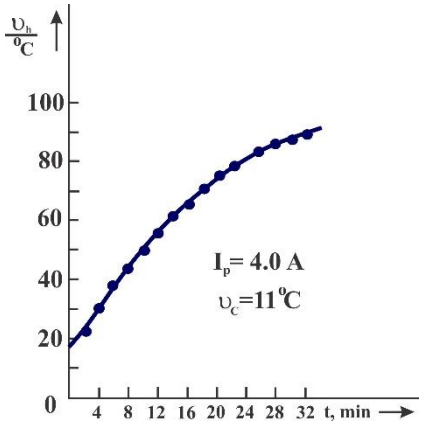

Figure 5 – The relationship of hot side temperature and time

Pump heating capacity can be computed from the slope of the curve in Figure 5, where the curve begins as a straight line or by the formula. To calculate the heating capacity and efficiency at constant current I_C and constant temperature on the cold side T_c, we need to consider the heat transfer processes involved in the pump's operation. The heating capacity can be determined by the electrical power input P_{el}, and the efficiency can be calculated using the output heating power Q and the electrical input power:

$$P_h = \frac{C_{tot}\Delta T_h}{\Delta T} \tag{10}$$

The corresponding efficiency score was calculated using formula 9, with $P_{el} = I_P * U_p$, corresponding results in Table 1.

Table 1 – Calculated results for pump heating

	m, kg	$C, \frac{J}{kg*K}$
Water	0.194	4182
Brass	0.0983	381
Copper block	0.712	383

$$C_{tot} = m_W * C_W + m_{Br} * C_W + m_{CU} * C_{CU} = 1121 \frac{J}{kg*K} \quad (11)$$

Through the slope on the graph of Figure 2 we also obtained $\frac{\Delta T_h}{\Delta T} = 6.7 * 10^{-2}$ and $P_h = 75\ W$. The efficiency at average values I_P of 4.0 A and U_P of 12.5 V was η_C = 1.5.

We also investigated the water temperature as a function of time, a graph of which can be seen in Figure 6. Measurements were taken for 24 seconds. The influence of the cooling mode on the result has led us to study this aspect. Figure 7 shows two curves relating the temperature of water that was subjected to hot-side cooling with an air cooler an air cooler (curve a) and cooled by convection (curve b), i.e. forced cooling.

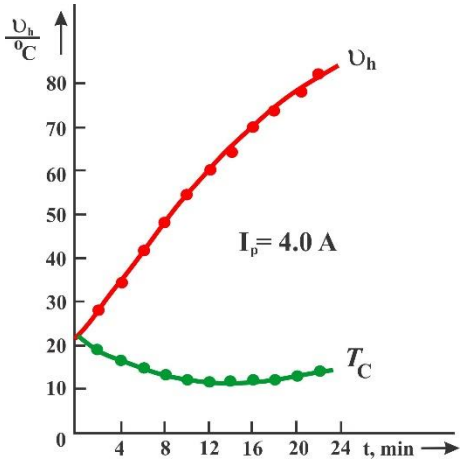

Figure 6 – T_w as a function of time

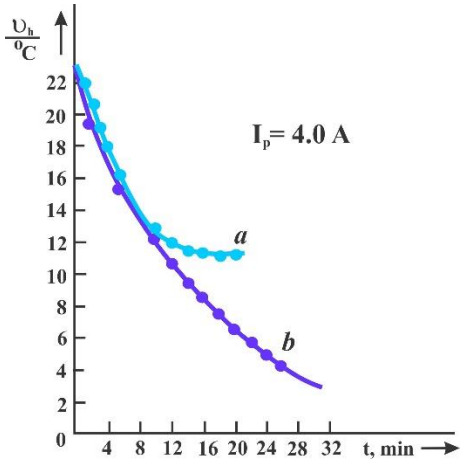

Figure 7 – T_w after using an air cooler to cool the hot side: *a*) convection cooling; *b*) forced cooling

P_h and P_C and η_h and η_C can be calculated from the slopes of the curves $\upsilon_h = f(t)$ and $\upsilon_c = f(t)$ the relevant heat capacities.

With $\frac{\Delta \upsilon_h}{\Delta t} = 0.056 \frac{K}{s}$ (start of curve) and $\frac{c \Delta \upsilon_C}{\Delta t} = -0.023 \frac{K}{s}$ and $C_{tot} = 1121 \frac{J}{K}$, we obtain: P_h = 63 W and P_C = 26 W. In the range considered U_P, the voltage was 12.4 V, so that we obtain the efficiency ratings $\eta_h = 1.3$ and $\eta_C = 0.52$ (I = 4 A, T = 22 °C).

The temperature changes that were seen in the cold side of the water bath when the hot side was cooled with an air cooler are depicted in Figure 7. After 20 minutes, the hot side temperature first dropped to about 72°C without the fan. When the maximum temperature differential was reached as a result of this decrease, the Peltier pump's power output decreased to zero. On the other hand, the hot side's temperature steadied after the fan was turned on, and after 20 minutes, it remained at about 45°C.

4. Conclusions

In conclusion, the experimental investigation of the Peltier heat pump has provided valuable insights into its cooling and heating capacities under specific operating conditions. By determining the cooling capacity as a function of the current, the efficiency of the pump in transferring heat from

the cooled system can be evaluated. The cooling capacity serves as a quantitative measure of the pump's ability to remove heat, which is essential for applications requiring precise temperature control, such as HVAC systems, refrigeration, or electronic device cooling.

In this study, the cooling capacity of the pump was determined to be 49 watts at a pump current of 5 amperes, where the input equaled the cooling power. This finding represents a significant parameter in assessing the effectiveness of the pump under specified operational parameters.

Furthermore, understanding the heating capacity of the pump is crucial for evaluating its performance in heating applications. The heating capacity quantifies the amount of heat the pump can generate under specific conditions. The plot of hot side temperature versus time allows for the computation of heating capacity from the slope of the curve. This information is vital for optimizing thermal management systems and heating devices utilizing Peltier heat pump technology.

To further analyze the heating capacity and efficiency at constant current and constant temperature on the cold side, the heat transfer processes involved in the pump's operation must be considered. Table 1 presents calculated results for pump heating, including specific heat capacities for different materials used in the experimental setup (water, brass, and copper block). These values facilitate the evaluation of heat transfer characteristics and efficiency within the Peltier heat pump system.

In summary, the experimental investigation outlined in this study contributes valuable data and insights into the operational capabilities and performance metrics of Peltier heat pumps, which are instrumental in advancing thermal management technologies for various industrial and consumer applications.

References

1. Experimental investigation of a novel thermal energy storage unit in the heat pump system / M. Koşan, M. Aktaş // Journal of Cleaner Production. — 2021. — Vol. 311. — P.127607. https://doi.org/10.1016/j.jclepro.2021.127607
2. Thermal performance evaluation of multi-tube cylindrical LHS system / B.G. Abreha, P. Mahanta, G. Trivedi // Applied Thermal Engineering. — 2020. — Vol. 179. — P. 115743 https://doi.org/10.1016/j.applthermaleng.2020.115743
3. Phase change storage solar heat pump hydronics based on cloud computing / W. WU // Thermal Science. — 2024. — Vol. 28, No. 2B. — P. 1423–1429. https://doi.org/10.2298/TSCI2402423W
4. Total energy heat pump / Y.H.V. Lun, S.L.D. Tung // Green Energy and Technology. — 2020. — P. 65–79. https://doi.org/10.1007/978-3-030-31387-6_5
5. Performance comparison of single-stage/cascade heat pump for waste heat recovery of printing-dyeing industry / D. Gu, Y. Yang, Y. Wu, W. Yan, B. Hu, L. Shi, C. Shen, M. Chen, C. Zheng, Y. Cai, W. Li // Second International Conference on Energy, Power, and Electrical Technology (ICEPET 2023). — 2023. — Vol. 12788. — P. 3004469. https://doi.org/10.1117/12.3004469
6. Analysis of a solar-assisted heat pump system with hybrid energy storage for space heating / S. Zhang, S. Liu, J. Wang, Y. Li, Z. Yu // Applied Thermal Engineering. — 2023. — Vol. 231. — P. 120884. https://doi.org/10.1016/j.applthermaleng.2023.120884
7. Peltier effect: From linear to nonlinear / Z. Yang, C. Zhu, Y.-J. Ke, X. He, F. Luo, J. Wang, J.-F. Wang, Z.-G. Sun // Wuli Xuebao/Acta Physica Sinica. — 2021. — Vol. 70, No. 10. — P. 1826. https://doi.org/10.7498/aps.70.20201826
8. Theoretical and Experimental Investigation about the Influence of Peltier Effect on the Temperature Loss and Performance Loss of Thermoelectric Generator / X. Li, J. Wang, Q. Meng, D. Yu // Energy Technology. — 2022. — Vol. 10, No. 4. — P. 895. https://doi.org/10.1002/ente.202100895
9. Improvement of the Self-Heating Performance of an Advanced SiGe HBT Transistor through the Peltier Effect / A. Boulgheb, M. Lakhdara, S. Latreche // IEEE Transactions on Electron Devices. — 2021. — Vol. 68, No. 2. — P. 479–484. https://doi.org/10.1109/TED.2020.3044869
10. Portable Thermal Electricity Generator Using the Seebeck Effect of Peltier as an Alternative Energy / Habibullah, Hastuti, T. Muhammad, D.S. Putra, J. Sardi // 2023 International Conference on Advanced Mechatronics, Intelligent Manufacture and Industrial Automation, ICAMIMIA 2023 – Proceedings. — 2023. — Vol. 1. — P. 564–568. https://doi.org/10.1109/ICAMIMIA60881.2023.10427831
11. Thermoregulation of Smart Clothing based on Peltier Elements / M.F. Mitsik, M.V. Byrdina // 2020 IEEE East-West Design and Test Symposium, EWDTS 2020 - Proceedings. — 2020. — Vol. 4. — P. 164143. https://doi.org/10.1109/EWDTS50664.2020.9224805
12. Peltier elements vs. heat sink in cooling of high power LEDs / N. Bădălan, P. Svasta // Proceedings of the International Spring Seminar on Electronics Technology. — 2015. — Vol. 2015 – September. — P. 124–128. https://doi.org/10.1109/ISSE.2015.7247975

12. Peltier elements vs. heat sink in cooling of high power LEDs / N. Bădălan, P. Svasta // Proceedings of the International Spring Seminar on Electronics Technology. — 2015. — Vol. 2015 – September. — P. 124–128. https://doi.org/10.1109/ISSE.2015.7247975
13. The central role of the Peltier coefficient in thermoelectric cooling / J. Garrido, A. Casanovas // Journal of Applied Physics. — 2014. — Vol. 115, No. 12. — P. 123517. https://doi.org/10.1063/1.4869776
14. Peltier modules in cooling systems for electronic components / K. Domke, P. Skrzypczak // Advanced Computational Methods and Experiments in Heat Transfer XI. — 2010. — Vol. 68. — P. 3–12. https://doi.org/10.2495/HT100011
15. Dismantling and chemical characterization of spent Peltier thermoelectric devices for antimony, bismuth and tellurium recovery / M. Balva, S. Legeai, L. Garoux, N. Leclerc, E. Meux // Environmental Technology (United Kingdom). — 2017. — Vol. 38, No. 7. — P. 791–797. https://doi.org/10.1080/09593330.2016.1211748
16. Direct observation of the spin-dependent Peltier effect / J. Flipse, F.L. Bakker, A. Slachter, F.K. Dejene, B.J. Van Wees // Nature Nanotechnology. — 2012. — Vol. 7, No. 3. — P. 166–168. https://doi.org/10.1038/nnano.2012.2

Information about authors:

Aliya Nurbayeva – Master Student, Faculty of Mechanical Engineering, Energy and Information Technologies, Akhmet Baitursynuly Kostanay Regional University, 47 Baytursynov st., Kostanay, Kazakhstan, alya.nurbayeva@mail.ru
Karina Mussabekova – Master Student, Faculty of Mechanical Engineering, Energy and Information Technologies, Akhmet Baitursynuly Kostanay Regional University, 47 Baytursynov st., Kostanay, Kazakhstan, karina.mussabekova@mail.ru

Authors Contribution:

Aliya Nurbayeva – concept, methodology, resources, data collection, testing, modeling.
Karina Mussabekova – analysis, visualization, interpretation, drafting, editing, funding acquisition.

Received: 01.05.2024
Revised: 03.05.2024
Accepted: 03.05.2024
Published: 03.05.2024